Ordered Magnetic Frustration

VII. Na$_2$NiFeF$_7$: Reexamination of Its Crystal Structure in the True Space Group after Corrections from Renninger Effect and Refinement of Its Frustrated Magnetic Structure at 4.2 and 55 K

Y. LALIGANT AND Y. CALAGE

Laboratoire des Fluorures (UA CNRS 449), Faculté des Sciences, Université du Maine Route de Laval, 72017 Le Mans Cedex, France

G. HEGER

Laboratoire Léon Brillouin 91191, Gif/Yvette Cedex, France

J. PANNETIER

ILL, Avenue des Martyrs, 156X, 38042 Grenoble Cedex, France

AND G. FEREY*

Laboratoire des Fluorures (UA CNRS 449), Faculté des Sciences, Université du Maine Route de Laval, 72017 Le Mans Cedex, France

A new refinement of the crystal structure at 300 K and of the magnetic structure at 4.2 and 55 K of the ferrimagnetic weberite Na$_2$NiFeF$_7$ is undertaken in order to fully reveal both the true space group of this compound and its magnetically frustrated character. The reflections which previously obliged us to choose space group *Imm2* are only due to Renninger effect. The true space group is *Imma* ($a = 7.2338(3)$ Å, $b = 10.3050(3)$ Å, $c = 7.4529(3)$ Å, $Z = 4$) at 300 K. The structure was refined from 1148 independent reflections to $R = 0.025$ ($R_w = 0.030$). The ferrimagnetic behavior is confirmed ($T_c = 88(2)$ K). Neutron powder diffraction shows that the nuclear and magnetic cells are identical and that there is an accident in the thermal evolution of the intensity of some magnetic peaks. Among the different modes given by the Bertaut's macroscopic theory, the best fit is obtained for both temperatures with the modes $-F_x$ and F_x, G_z for Fe^{3+} and Ni^{2+} sublattices, respectively, instead of $-F_x$ and $+F_x$ in the solution previously proposed by Heger. The corresponding moments are 4.93(11) and 1.36(21) μ_B at 4.2 K ($R_{mag} = 0.045$) and 4.34(12) and 0.97(22) μ_B at 55 K ($R_{mag} = 0.052$). The slight anomaly in the thermal variation of the intensity of some magnetic reflections at 50 K is due to a significant change in the spin canting at this temperature, without any modification of the magnetic modes. A Mössbauer study confirms the anomaly from the thermal variation of the magnetic hyperfine field at the Fe nucleus. © 1989 Academic Press, Inc.

---

[1] To whom correspondence should be addressed.

Introduction

For several years, we have focused our attention on the problem of antiferromagnetism on a triangular sublattice of magnetic cations in fluorides (*1–6*) in order to illustrate the concept of frustration introduced by Toulouse (*7*). Our previous studies on $M^{2+}Fe^{3+}F_5(H_2O)_2$ (*8–10*) (M^{2+} = Mn, Fe, Zn) showed that their crystal structure is closely related to the weberite type, represented by Na_2NiFeF_7. The two structures differ by an inversion of M^{2+} and M^{3+} sites. If the space group of the inverse weberites is now well established (*6, 8, 10*), that of the direct weberites remains questionable (*11–14*). Previous structural papers claim either space group *Imma* (*12*) or *Imm2* (*11, 13, 14*). Moreover, the frustrated magnetic structures of $MFeF_5(H_2O)_2$ are relatively complex (*5, 6*), with important spin cantings. Surprisingly, this is not the case for Na_2NiFeF_7 (*15*). These differences were the motivation of our reexamination of both the nuclear and the magnetic structures of the latter compound.
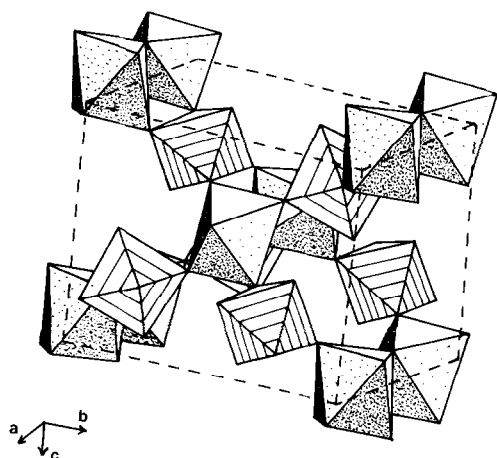

FIG. 1. Perspective view of the structure of Na₂Ni FeF₇. Ni²⁻ and Fe³⁻ octahedra are dot shaded and hatched, respectively.

The crystal and magnetic structures of the ferrimagnet Na_2NiFeF_7 (T_c = 88(2) K (*15–18*)) were previously studied by Haegele *et al.* (*13*) and Heger and Viebahn-Hansler (*15*), respectively. At room temperature, the crystal structure was solved using the space group *Imm2* (a = 7.245(1) Å, b = 10.320(2) Å, c = 7.458(1) Å, Z = 4 at 300 K) because of the existence of very weak reflections ($hk0$) with $h = 2n + 1$. However, it is worthy to note that it was not verified that these reflections could originate from Renninger effect (*19*). The structure of the weberite can be described from hexagonal tungsten bronze-like (HTB) planes linked one to the other by isolated FeF_6 octahedra (Fig. 1). The (HTB) planes are built up from separate *trans* chains of corner-sharing octahedra of Ni^{2+} and other FeF_6 octahedra which link the chains by four of their corners. In the resulting HTB plane, the cationic subnetwork draws triangles, and can lead to frustration effects. The magnetic structure (*15*), previously solved at 4.2 K from six reflections corresponding to 18 *hkl* triplets could be described by two ferromagnetic sublattices of Ni^{2+} and Fe^{3+} coupled antiferromagnetically, all the spins being along [100]. Moreover, in the paper by Heger, the thermal evolution of the intensity of the (101) magnetic reflection seemed to exhibit an accident at 50 K, perhaps indicative of a change in the magnetic structure. The ambiguity concerning the existence of ($hk0$) reflections with $h = 2n + 1$ and the large improvement of neutron powder diffraction techniques since the previous paper lead us to reexamine in a first step the crystal structure at 300 K in the true space group, and then the magnetic structure of Na_2NiFeF_7 at 4.2 and 55 K. This last study requires us first to explain precisely the orientation of the spins, especially for Ni^{2+} for which the Kanamori–Goodenough rules (*20, 21*) predict only antiferromagnetic coupling, and also to try to explain the anomaly at 50 K.

	Cell parameters[a]
Symmetry: orthorhombic	
Systematic extinctions:	$a = 7.2338(3)$
(hkl): $h + k + l = 2n + 1$	$b = 10.3050(3)$
$(hk0)$: $h = 2n + 1$	$c = 7.4529(2)$
Space group: $Imma$	$V = 555.57$ Å^3
$\rho_{exp} = 3.50$ g cm^{-3}	$Z = 4$
$\rho_{calc} = 3.49(1)$ g cm^{-3}	

[a] Refined from 24 reflections and calibrated with Ge standard.

Experimental

Single crystals for x-ray determination were grown by a flux method previously described (22–24). Because of the difficulty of obtaining by direct synthesis a pure powder of Na_2NiFeF_7 free of chiolite $Na_5Fe_3F_{14}$ and $NaNiF_3$, powder samples were obtained by grinding single crystals.

A second harmonic generation measurement on the ground crystals gave a negative, and thus inconclusive, result. A well-shaped single crystal was selected by optical examination and then transformed into a sphere ($R = 0.067$ mm). X-ray data were then collected using an AED-2 Siemens-Stoe four-circle diffractometer. After calibration with a germanium sphere, lattice constants were determined from 24 reflections by the double scan ($+\omega, +2\theta$; $-\omega, -2\theta$) technique. The corresponding values are listed in Table I. Before any routine collection of data, the body centering was tested from 335 reflections ($0 \le h \le 6$, $0 \le k \le 9$, $0 \le l \le 7$) and a series of weak reflections ($hk0$) with $h = 2n + 1$, previously observed by Haegele et al. (13) and which led them to propose the space group $Imm2$, were systematically checked by so-called ψ-scan rotation. As it will be discussed later, they are only due to Renninger effect; therefore, the intensity

collection was made further with the conditions of space group $Imma$ in the four following octants: (hkl), $(-h,-k,l)$, $(h,-k,-l)$, and $(-h,k,-l)$ with $h_{max} = 14$, $k_{max} = 20$, $l_{max} = 14$. This corresponds to an angular range $2° < \theta < 45°$. Other experimental details are given in Table II.

The intensities were corrected from Lorentz polarization and absorption. After averaging, the structure refinement was performed using the SHELX program (25). Ionic scattering factors and anomalous dispersion parameters were taken from the "International Tables for X-Ray Crystallography" (26). The refinement converged rapidly to the values given in Table III. A table of structure factors will be supplied by G.F. upon request.

Neutron diffraction patterns were first rapidly collected at several temperatures below $T_c = 88(2)$ K on the D1B powder diffractometer of the HFR of the Institut Laue-Langevin (Grenoble), using a wavelength of 2.519 Å, in order to confirm the slight anomaly on the thermal variation of the (101) peak at 50 K. Always on D1B, longer exposures were then realized at 55 K, i.e., just above the accident, and at 4.2 K in order to obtain accurate data for further refinements. Higher harmonic wavelengths were suppressed by a set of pyrolytic graphite filters. The sample was inserted in a cylindrical vanadium can ($\phi = 10$ mm) held in a vanadium tailed cryostat. The data were collected in the range $10° < \theta < 50°$ and correspond to 43 hkl triplets. Their analysis was performed with the Rietveld profile refinement method (27), as modified by Hewat (28). The nuclear scattering lengths and magnetic form factors were taken from (29) and (30), respectively.

^{57}Fe Mössbauer experiments were performed in the usual way over the temperature range 4.2–300 K. Mössbauer samples contained 5–6 mg/cm^3 of natural iron and a constant acceleration spectrometer was

TABLE II

CONDITIONS OF INTENSITY DATA COLLECTION
AND REFINEMENT

Crystal size: sphere R = 0.067 mm
Radiation: Mo$K\alpha$ (λ = 0.71069 Å)
Scan mode: $\omega - 2\theta$ with profile fitting data collection
Step scan range: 0.9661–0.0139 tg(θ)
Detector aperture (mm): 5
θ_{min}: 2°
θ_{max}: 45°
Range of measurement: $-14 < h < 14$
$\qquad\qquad\qquad\qquad -20 < k < 20$
$\qquad\qquad\qquad\qquad -14 < l < 14$
Standard reflections: 0   3   1 ⎫
$\qquad\qquad\qquad\quad$ 1   0   3 ⎬ measured every 45 min
$\qquad\qquad\qquad\quad$ 2   1   1 ⎭
Intensity variation max: 3%
Reflections measured (without standards): 5277
Reflections rejected ($F/\sigma(F) > 6$): 13
Independent reflections: 1184
R (from averaging): 0.0190
Absorption correction: Program EMPIR (Stoe and Cie, 1986)
Absorption coefficient: 62.48 cm^{-1} (Mo$K\alpha$)
Transmission factors max: 0.695
$\qquad\qquad\qquad\qquad$ min: 0.549
F magnitudes used in least-squares refinement
Shift/esd mean: 0.002
$\qquad\qquad\quad$ max: 0.009

used in the triangular mode with a 25-mCi source of Rh : ^{57}Co. Data were refined with the program MOSFIT (31).

Single-Crystal X-Ray Diffraction

As mentioned under "Introduction," the first aim of this study was the determination of the correct space group of the direct weberite after correction from Renninger effect (19). Indeed, the only physical argument supporting the noncentrosymmetric space groups was the observation of several very weak ($hk0$) reflections with $h = 2n + 1$. Our routine intensity collection on the weberite Na$_2$NiFeF$_7$ produced also 13 very weak ($hk0$) reflections with $h = 2n + 1$ and $I/\sigma(I) > 3$. However, one may not rule out the possibility of double reflection (19) to explain the existence of these weak reflec-

tions, a point which was not considered by Haegele et al. (13) and Knop et al. (14).

As the occurrence of a specific double reflection requires a combination of particular wavelength with an orientation of the reciprocal lattice, the existence of a Renninger effect can be checked either, for a given orientation, by changing the wavelength, or, alternatively, for a given wavelength, by changing the orientation of the crystal. A series of ($hk0$) reflections with $h = 2n + 1$ was then tested by so-called ψ-scan rotation on a AED-2 four-circle diffractometer, and we were able to prove that there is some probability for Renninger effect in the case of the weberite structure and Mo$K\alpha$ radiation. In Fig. 2, the integrated background corrected intensity of the (110) reflection is drawn as a function of ψ-rotation. It is obvious that there are many

TABLE III

REFINED ATOMIC COORDINATES AND THERMAL PARAMETERS[a,b] OF
Na_2NiFeF_7 (R_F = 0.029, R_{wF} = 0.034)

Atom	x	y	z	U_{11}	U_{22}	U_{33}	U_{23}	U_{13}	U_{12}
Na1	0	0	0	236(6)	568(11)	190(5)	189(5)	0	0
Na2	$\frac{1}{4}$	$\frac{1}{4}$	$\frac{3}{4}$	223(7)	230(7)	667(14)	0	−36(5)	0
Ni^{2+}	$\frac{1}{4}$	$\frac{1}{4}$	$\frac{1}{4}$	68(1)	66(1)	82(1)	0	11(1)	0
Fe^{3+}	0	0	$\frac{1}{2}$	90(1)	84(1)	83(1)	25(1)	0	0
F1	0	$\frac{1}{4}$	0.1473(2)	74(3)	286(6)	177(4)	0	0	0
F2	0	0.4109(1)	0.7299(1)	229(4)	207(4)	109(2)	16(1)	0	0
F3	0.1960(1)	0.3840(1)	0.4348(1)	162(2)	188(2)	290(2)	−108(2)	11(1)	51(1)

[a] Standard deviations given in parenthesis. U_{ij} are ×10^4.

[b] The vibrational coefficients relate to the expression: T = exp$[-2\pi^2(h^2a^{*2}U_{11} + k^2b^{*2}U_{22} + l^2c^{*2}U_{33} + 2hka^*b^*U_{12} + 2hla^*c^*U_{13} + 2klb^*c^*U_{23})]$.

configurations where the observed intensity is much higher than the marked limit of $3\sigma(I)$. In all cases, a small ψ-rotation around the scattering vector yields a complete vanishing of the diffracted intensity (an example is given in Fig. 3), and leads us to choose the space group *Imma* (No. 74) to refine the structure.

This refinement converges to a reliability factor (R = 0.025, R_w = 0.030) slightly lower than that of Haegele with more than twice the number of reflections (1148 in this work; 529 for (*13*)). The results of the refinement are given in Table III and the characteristic distances and angles in Table IV. Despite a change of space group, the crys-

tal chemistry of the direct weberite structure obviously remains the same as described under "Introduction."

However, one should not conclude from this study that all direct weberites crystallize in space group *Imma*. Indeed, we were
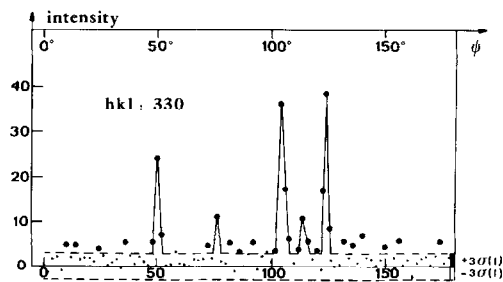

FIG. 2. Integrated background corrected intensity of (3 3 0) as a function of ψ rotation around the scattering vector.
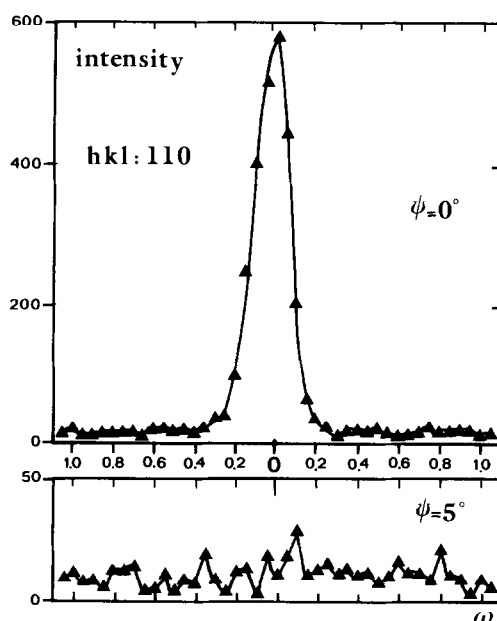

FIG. 3. Evolution of the intensity of (1 1 0) with a ψ rotation of 5° around the scattering vector.

TABLE IV

INTERATOMIC DISTANCES (Å) AND ANGLES (°) IN Na$_2$NiFeF$_7$
(STANDARD DEVIATIONS ARE GIVEN IN PARENTHESES)

	Ni^{2+} octahedron		
Ni–F1	2 × 1.9655(3)	F1–Ni–F1	180.00(2)
Ni–F3	4 × 1.9877(9)	F1–Ni–F3	4 × 95.22(5)
⟨Ni–F⟩	1.9803 (D_{Shannon} = 1.975)	F1–Ni–F3	4 × 84.78(5)
		F3–Ni–F3	2 × 180.00(9)
		F3–Ni–F3	2 × 91.99(9)
		F3–Ni–F3	2 × 88.10(9)

	Fe^{3+} octahedron		
Fe–F2	2 × 1.9408(8)	F2–Fe–F2	180.00(4)
Fe–F3	4 × 1.9186(9)	F2–Fe–F3	4 × 94.04(5)
⟨Fe–F⟩	1.9258 (D_{Shannon} = 1.933)	F2–Fe–F3	4 × 85.96(5)
		F3–Fe–F3	2 × 180.00(9)
		F3–Fe–F3	2 × 84.58(9)
		F3–Fe–F3	2 × 95.42(9)

Superexchange angles and metal–metal distances

Ni–Ni	2 × 3.6169(3)	Ni–F1–Ni	133.88(2)
Ni–Fe	4 × 3.6578(3)	Ni–F3–Fe	138.90(2)

Sodium polyhedra

Bipyramid: Na1		Prism: Na2	
Na1–F1	2 × 2.7986(3)	Na2–F2	4 × 2.4590(9)
Na1–F2	2 × 2.2148(8)	Na2–F3	4 × 2.7539(9)
Na1–F3	4 × 2.5487(8)		
F1–Na1–F1	180.00(2)	F2–Na2–F2	2 × 180.00(4)
F1–Na1–F2	2 × 91.47(4)	F2–Na2–F2	2 × 84.87(4)
F1–Na1–F2	2 × 88.53(4)	F2–Na2–F2	2 × 95.14(4)
F1–Na1–F3	2 × 59.57(4)	F2–Na2–F3	2 × 60.31(7)
F1–Na1–F3	4 × 120.43(4)	F2–Na2–F3	4 × 100.45(7)
F2–Na1–F2	180.00(7)	F2–Na2–F3	4 × 119.69(7)
F2–Na1–F3	4 × 91.15(7)	F2–Na2–F3	4 × 79.55(7)
F2–Na1–F3	4 × 88.85(7)	F3–Na2–F3	2 × 180.00(9)
F3–Na1–F3	2 × 60.86(9)	F3–Na2–F3	2 × 119.81(9)
F3–Na1–F3	2 × 119.14(9)	F3–Na2–F3	2 × 60.19(9)
F3–Na1–F3	2 × 180.00(9)		

very recently informed of an unpublished structural work (*32*) on Na$_2$NiAlF$_7$. In this study, it is clearly proved by ψ-scan that (*hk*0) reflections with $h = 2n + 1$ do not originate from Renninger effect and are intrinsic to the structure (SG $I2_12_12_1$), in agreement with previous nonlinear optical measurements (*33*). Therefore, the only possible answer to the question of Knop *et al.* (*14*) "What is the true space group of weberite?" might be "Weberites crystal-lize in several space groups," and this may depend on the size of the tervalent ion.

Neutron Powder Diffraction and Mössbauer Study

Below T_c, new magnetic peaks appear: they can be indexed in the nuclear cell with the same I lattice. The study of the thermal evolution of the intensity of some peaks
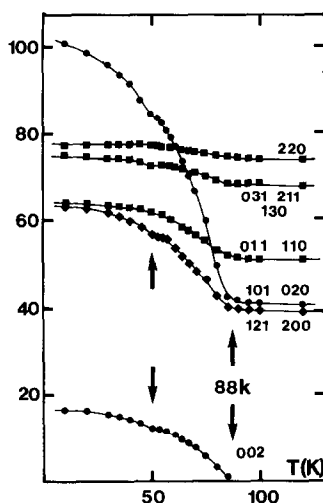
FIG. 4. Thermal variation of the intensity of a few reflections measured by neutron powder diffraction. The error bars correspond to the dimension of the squares and circles at $T < 60$ K.

also confirms the presence of an anomaly at 50 K (Fig. 4).

The identity of the nuclear and magnetic cells allows Bertaut's macroscopic theory to be used (34). 2_x, 2_y, -1, and I translation are taken as the four independent symmetry elements. If R_i and S_i ($i = 1, 4$) are the magnetic moments of Fe^{3+} and Ni^{2+} corresponding to the atomic coordinates reported in Table V, it is possible to define in each sublattice four linear combinations of the moments $F = M_1 + M_2 + M_3 + M_4$, $G = M_1 - M_2 + M_3 - M_4$, $C = M_1 + M_2 - M_3 - M_4$, $A = M_1 - M_2 - M_3 + M_4$ ($M = R, S$) which represent the ferromagnetic and antiferromagnetic modes of coupling. The base vectors, in the irreducible representation of space group $Imma$ lead to 16 modes, but only 3 of them (Γ_2, Γ_3, and Γ_4) are compatible with the magnetization of

TABLE V

ATOMIC COORDINATES OF THE SPINS OF Ni^{2+} (R_i) AND Fe^{3+} (S_i) AND CORRESPONDING MAGNETIC MODES IN SPACE GROUP $Imma$

			Ni^{2+}				Fe^{3+}		
R_1	$\frac{1}{4}$	$\frac{1}{4}$	$\frac{1}{4}$	S_1	0	0	$\frac{1}{2}$		
R_2	$\frac{3}{4}$	$\frac{1}{4}$	$\frac{1}{4}$	S_2	0	$\frac{1}{2}$	$\frac{1}{2}$		
R_3	$\frac{3}{4}$	$\frac{3}{4}$	$\frac{3}{4}$	S_3	$\frac{1}{2}$	$\frac{1}{2}$	0		
R_4	$\frac{1}{4}$	$\frac{3}{4}$	$\frac{3}{4}$	S_4	$\frac{1}{2}$	0	0		

Mode	2_x	2_y	-1	I						
$\Gamma 1$	$+$	$+$	$+$	$+$	.	G_y	.	G_x	.	.
$\Gamma 2$	$-$	$+$	$+$	$+$	.	F_y	.	.	F_y	G_z
$\Gamma 3$	$+$	$-$	$+$	$+$	F_x	.	G_z	F_x	.	.
$\Gamma 4$	$-$	$-$	$+$	$+$	G_x	.	F_z	.	G_y	F_z
$\Gamma 5$	$+$	$+$	$-$	$+$	.	.	.	.	.	.
$\Gamma 6$	$-$	$+$	$-$	$+$	.	.	.	.	.	.
$\Gamma 7$	$+$	$-$	$-$	$+$	.	.	.	.	.	.
$\Gamma 8$	$-$	$-$	$-$	$+$	.	.	.	.	.	.
$\Gamma 9$	$+$	$+$	$+$	$-$	.	.	.	C_x	.	.
$\Gamma 10$	$-$	$+$	$+$	$-$	.	.	.	.	A_y	C_z
$\Gamma 11$	$+$	$-$	$+$	$-$	.	.	.	A_x	.	.
$\Gamma 12$	$-$	$-$	$+$	$-$	.	.	.	.	C_y	A_z
$\Gamma 13$	$+$	$+$	$-$	$-$	C_y	.	.	.	.	.
$\Gamma 14$	$-$	$+$	$-$	$-$	.	A_y	.	.	.	.
$\Gamma 15$	$+$	$-$	$-$	$-$	A_x	.	C_z	.	.	.
$\Gamma 16$	$-$	$-$	$-$	$-$	C_x	.	A_z	.	.	.

TABLE VI

CELL PARAMETERS AND ATOMIC COORDINATES OF
Na₂NiFeF₇ AT 4.2 K IN SPACE GROUP *Imma*
(VALUES IN BRACKETS CORRESPOND TO THE
REFINEMENT AT 55 K)

$a = 7.203(1)$ Å, $b = 10.255(1)$ Å, $c = 7.429(1)$ Å
[7.203(1)]   [10.256(1)]   [7.429(1)]

Atom	x	y	z	B
Na1	0	0	0	1.2
				[1.5]
Na2	$\frac{1}{4}$	$\frac{1}{4}$	$\frac{3}{4}$	1.2
				[1.5]
Ni²⁺	$\frac{1}{4}$	$\frac{1}{4}$	$\frac{1}{4}$	0.15
				[0.25]
Fe³⁺	0	0	$\frac{1}{2}$	0.15
				[0.25]
F1	0	$\frac{1}{4}$	0.143(2)	0.35
			[0.146(2)]	[0.50]
F2	0	0.417(1)	0.733(2)	0.35
		[0.416(1)]	[0.734(2)]	[0.50]
F3	0.196(1)	0.377(1)	0.429(1)	0.35
	[0.196(1)]	[0.376(1)]	[0.428(1)]	[0.50]

both Fe³⁺ and Ni²⁺ sublattices and also with ferrimagnetism (Table V).

Starting from the 300 K atomic coordinates of Table III, the refinement concerned both atomic coordinates and magnetic moments. The best fit ($R_{nuc} = 0.047$, $R_{mag} = 0.045$ at 4.2 K; $R_{nuc} = 0.048$, $R_{mag} = 0.052$ at 55 K) between observed and calculated intensities correspond to the Γ_3 mode: $+F_x, +G_z$, and $-F_x$ for Ni²⁺ and Fe³⁺ components respectively (this mode is also allowed with space group *Imm*2). All other combinations of signs lead to an increase of the magnetic R factor, as does the solution previously proposed by Heger ($R_{mag} = 0.058$ at 4.2 K and 0.088 at 55 K). The atomic coordinates, the characteristic distances, and the components of the magnetic moments R and S on the axes of the cell are listed in Tables VI and VII, respectively. The comparison of the observed and calculated profiles appear in Fig. 5. The model proposed by Heger is roughly confirmed, but explained since the G_z component on the Ni sublattice has a significant value which leads to a spin canting of 36.9° (4.2 K) and 54.2° (55 K) between the Ni spins. Ferrimagnetism results from the opposite signs of F_x components of Fe³⁺ and Ni²⁺. The resulting calculated moment ($\mu = 3.70$ μ_B) is larger than the moment previously obtained from single-crystal magnetization measurements ($\mu = 2.3$ μ_B) with a magnetic field parallel to the a axis (*17*). Table VIII presents the contribution of each magnetic sublattice to the magnetic dipolar energy, the lattice summation being carried out in the real space within a sphere of 100 Å radius.

TABLE VII

REFINED VALUES OF THE COMPONENTS OF THE MAGNETIC
MOMENTS AT $T = 4.2$ AND 55 K IN THE MODE Γ_3

	Ni²⁺				Fe³⁺			
T (K)	R_x	R_y	R_z	$\|R\|$	S_x	S_y	S_z	$\|S\|$
4.2	1.29	.	0.43	1.36	−4.93	.	.	4.93
	(12)		(20)		(11)			
55.0	0.86	.	0.44	0.97	−4.34	.	.	4.34
	(14)		(20)		(12)			

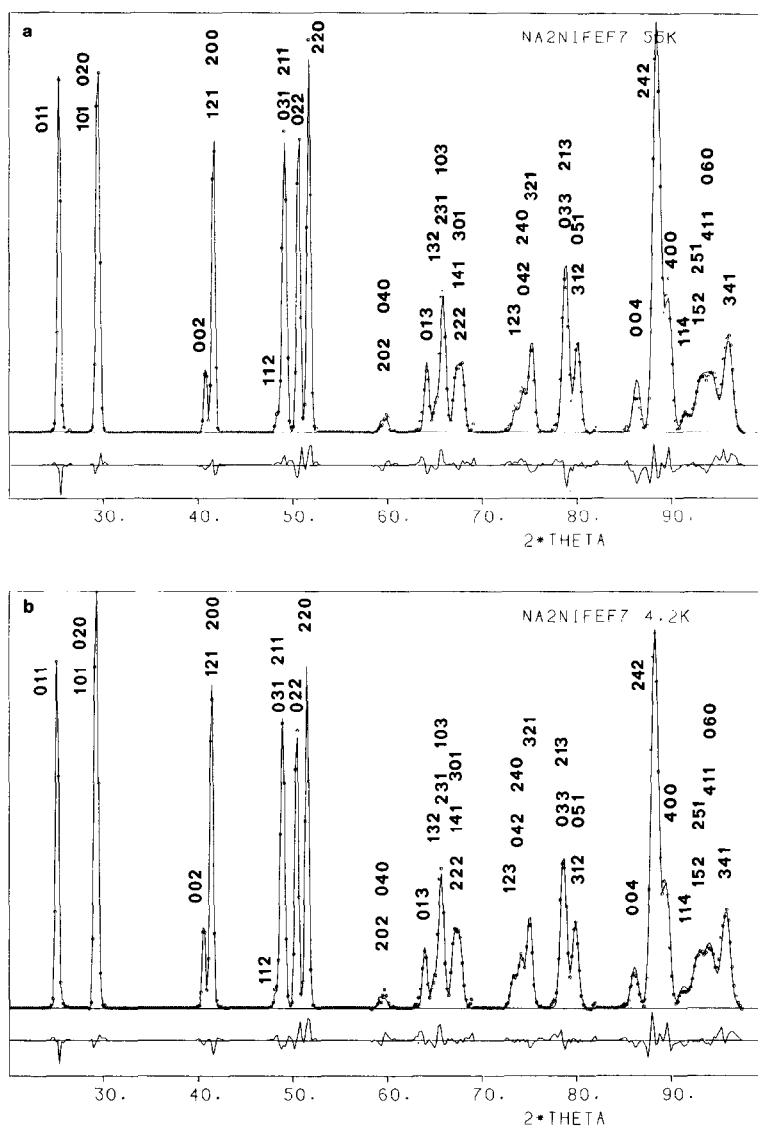| T (K)	R_p	R_{wp}	R_{nuc}	R_{mag}
4.2	0.079	0.083	0.047	0.045
55.0	0.083	0.084	0.048	0.052

FIG. 5. Comparison of observed and calculated intensities of Na_2NiFeF_7 at 55 K (a) and 4.2 K (b).

From the above results, the anomaly at 50 K does not arise from a magnetic phase transition but only from a small reorientation of the Ni^{2+} spins. It is due to the increase of the F_x component when temperature decreases, whereas G_z remains constant in the temperature range 55–4.2 K.

The existence of this accident had to be confirmed by Mössbauer spectroscopy. Mössbauer spectra of Na_2NiFeF_7 at 300 and 5 K were previously published by Pebler et al. (35); however, in this paper, they mentioned neither the values of the fitted data nor the study of their evolution with temperature. Therefore, we have undertaken a

TABLE VIII

Magnetic Dipolar Energy (J mole^{-1})
(Values of 55 K in Parentheses)

Contribution from → on ↓	Ni^{2+}	Fe^{3+}	Ni^{2+} + Fe^{3+}
Ni^{2+}	−0.221	−0.251	−0.472
	(−0.074)	(−0.208)	(−0.283)
Fe^{3+}	−0.251	0.032	−0.219
	(−0.208)	(0.026)	(−0.183)

Fig. 7. Thermal variation of the paramagnetic fraction F_p of Na$_2$NiFeF$_7$.

new Mössbauer study of this compound at several temperatures, particularly in the vicinity of 50 K.

Mössbauer spectra at 300, 77, and 4.2 K are shown in Fig. 6 and fitted data at several temperatures are given in Table IX. The paramagnetic spectrum at room tem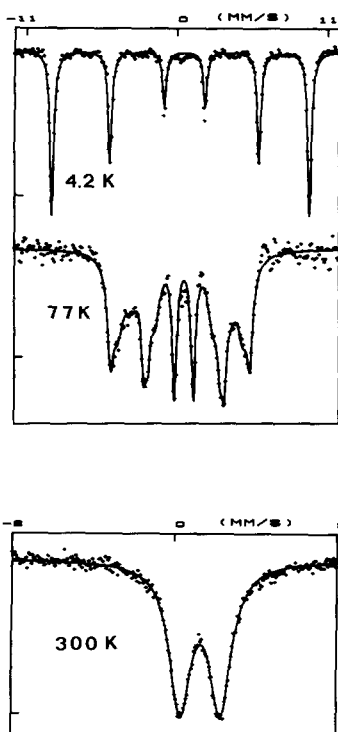perature consists of a well-resolved doublet; the isomer shift is very close to that obtained in the inverse weberites (*36, 37*), but the quadrupole splitting is sizeably smaller.

The Zeeman sextet begins to appear below 90 K. At 77 K, the spectrum is still poorly resolved and was fitted using a hyperfine field distribution. Moreover, the thermal scanning of the paramagnetic line (Fig. 7) shows that the magnetic transition takes place over a relatively large range of temperature ($T = 10$ K). Both phenomena might suggest a small cationic disorder. The T_c value of 84(2) K deduced from the thermal scan compares well to that obtained by neutron diffraction.

At lower temperatures, sharper lines are

Fig. 6. Mössbauer spectra of Na$_2$NiFeF$_7$ at 300, 77, and 4.2 K.

TABLE IX

Mössbauer Data of Na$_2$NiFeF$_7$

T (K)	δ (mm sec^{-1})[a]	ΔE_Q ou 2ε[b] (mm sec^{-1})	H (kOe)	Γ (mm sec^{-1})
300	0.444(4)	0.494(4)	—	0.32(1)
100	0.529(4)	0.525(4)	—	0.38(1)
77	0.54(1)	−0.26(2)	290	0.10
65	0.56(1)	−0.26(2)	438(2)	0.66(1)
55	0.54(1)	−0.27(2)	483(2)	0.52(1)
50	0.55(1)	−0.27(2)	504(2)	0.48(1)
45	0.51(1)	−0.29(2)	527(2)	0.40(1)
40	0.54(1)	−0.27(2)	544(2)	0.40(1)
20	0.55(1)	−0.26(2)	578(2)	0.36(1)
4.2	0.54(1)	−0.27(2)	584(2)	0.34(1)

[a] Isomer shift relative to metallic iron at 300 K.
[b] Quadrupolar splitting of the external lines of the Zeeman spectrum.

observed for the Zeeman sextet. The thermal variation of the hyperfine field at Fe nucleus is shown in Fig. 8. A kink at 52 K is indeed observed, which corresponds to the change in the direction of the Ni spins, already observed by neutron diffraction. However, the quadrupole shift remains independent of the temperature, which indicates, in a first approximation, that the angle θ between the principal axis of the electric field gradient (EFG) and the hyperfine field doesn't change. This is in agreement with the neutron diffraction results, since Fe^{3+} moments lie along the **a** parameter whatever the temperature.

The critical exponent β was obtained from accurate measurements of the hyperfine field close to the magnetic ordering temperature T_c. Using $T_c = 84(2)$ K, as determined above, the critical law

$$H_{hf}(T)/H_{hf}(0) = D * ((T_c - T)/T_c)^\beta$$

was fitted to the experimental data, yielding

$$\beta = 0.30(1) \quad \text{and} \quad D = 1.02(3).$$

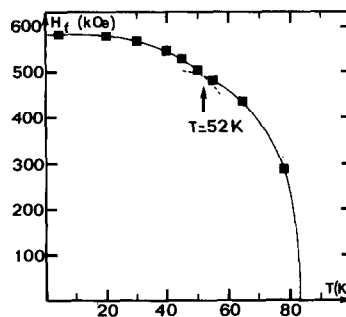This value of β is consistent with the 3D magnetic character of this compound.

FIG. 8. Thermal variation of the magnetic hyperfine field H_f. The error bars correspond to the dimensions of the squares.

of isolated linear chains of paramagnetic Ni^{2+} (therefore unfrustrated), a three-dimensional triangular magnetic subnetwork characterizes Na_2NiFeF_7 and leads to frustration. As previously proposed by Heger and Viebahn-Hansler (15) and Tressaud et al. (17), $Ni^{2+}-Fe^{3+}$ antiferromagnetic interactions are predominant and govern the exchange. They oblige the spins of Ni^{2+} to adopt, despite the negative value of their exchange interval, a frustrated parallel arrangement.

Conclusion

The two most prominent results of this study are the following. First, the ambiguity concerning the space group of the weberite Na_2NiFeF_7 is definitively suppressed. Second, the quasi-parallel arrangement of Ni^{2+} spins is quantitatively described and provides a clear example of the frustration of an antiferromagnetic coupling. The latter, predicted by the Kanamori–Goodenough rules for d^8-d^8 180° superexchange interactions, was already observed for the weberite Na_2NiAlF_7 (38); the substitution of paramagnetic Fe to diamagnetic Al modifies the dimensionality of the magnetic subnetwork. Whereas in Na_2NiAlF_7 the magnetic sublattice consists

References

1. G. FEREY, R. DE PAPE, AND B. BOUCHER, *Acta Crystallogr. Sect. B* **34**, 1084 (1978).
2. G. FEREY, M. LEBLANC, R. DE PAPE, AND J. PANNETIER, *Solid State Commun.* **53**(6), 559 (1985).
3. G. FEREY, M. LEBLANC, R. DE PAPE, AND J. PANNETIER, in "Inorganic Fluorides: Chemistry and Physics" (P. Hagenmuller, Ed.), p. 395, Academic Press, Orlando, FL (1985).
4. Y. LALIGANT, M. LEBLANC, J. PANNETIER, AND G. FEREY, *J. Phys. C* **19**, 1081 (1986).
5. M. LEBLANC, J. PANNETIER, R. DE PAPE, AND G. FEREY, *Solid State Commun.* **58**, 171 (1986).
6. Y. LALIGANT, J. PANNETIER, AND G. FEREY, *J. Solid State Chem.* **66**, 242 (1987).
7. G. TOULOUSE, *Commun. Phys.* **2**, 115 (1977).
8. W. HALL, S. KIM, J. ZUBIETA, E. G. WALTON, AND D. B. BROWN, *Inorg. Chem.* **16**, 1884–1887 (1977).

9. Y. LALIGANT, J. PANNETIER, P. LABBE, AND G. FEREY, *J. Solid State Chem.* **62**, 274 (1986).

10. Y. LALIGANT, J. PANNETIER, M. LEBLANC, P. LABBE, AND G. FEREY, *Z. Kristallogr.* **181**, 1 (1987).

11. A. BYSTRÖM, *Ark. Kemi. Mineral. Geol.* **18**, 10 (1944).

12. G. GUISEPPETTI AND C. TADINI, *Tschermaks Mineral. Petrogr. Mitt.* **25**, 57 (1978).

13. R. HAEGELE, W. VERSCHAREN, D. BABEL, J. M. DANCE, AND A. TRESSAUD, *J. Solid State Chem.* **24**, 77 (1978).

14. O. KNOP, T. S. CAMERON, AND K. JOCHEM, *J. Solid State Chem.* **43**, 213 (1982).

15. G. HEGER, AND R. VIEBAHN-HANSLER, *Solid State Commun.* **11**, 1119 (1972).

16. R. COSIER, A. WISE, A. TRESSAUD, J. GRANNEC, R. OLAZCUAGA, AND J. PORTIER, *C.R. Acad. Sci. (Paris) Ser. C* **271**, 142 (1970).

17. A. TRESSAUD, J. M. DANCE, J. PORTIER, AND P. HAGENMULLER, *Mater. Res. Bull.* **9**, 1219 (1974).

18. A. TRESSAUD, J. M. DANCE, M. VLASSE, AND J. PORTIER, *C.R. Acad. Sci. (Paris) Ser. C* **282**, 1105 (1976).

19. M. RENNINGER, *Z. Phys.* **106**, 141 (1937).

20. J. KANAMORI, *J. Phys. Chem. Solids* **10**, 87 (1959).

21. J. B. GOODENOUGH, "Magnetism and the Chemical Bond," Interscience, New York (1963).

22. J. NOUET, C. JACOBONI, J. Y. GERARD, G. FEREY, AND R. DE PAPE, *J. Cryst. Growth* **8**, 131 (1971).

23. J. P. MIRANDAY, Thèse, Le Mans (1972).

24. A. TRESSAUD AND J. M. DANCE, *Adv. Inorg. Chem.* **20**, 133 (1971).

25. G. SHELDRICK, "SHELX: A Program for Crystal Structure Determination," University of Cambridge (1976).

26. "International Tables for X-Ray Crystallography," Vol. IV, Kynoch Press, Birmingham (1974).

27. H. M. RIETVELD, *J. Appl. Crystallogr.* **2**, 65 (1969).

28. A. W. HEWAT, Harwell Report AERE, R 7350 (1973); *Acta Crystallogr. Sect.* **35**, 248 (1979).

29. L. KOSTER, AND H. RAUCH, IAEA contract 2517/RB (1981).

30. R. E. WATSON AND J. FREEMAN, *Acta Crystallogr.* **14**, 27 (1961).

31. J. TEILLET AND F. VARRET, Program MOSFIT, unpublished.

32. R. SCHMIDT, Dissertation, Marburg (1985).

33. A. TRESSAUD, L. LOZANO, AND J. J. RAVEZ, *Fluorine Chem.* **19**, 61 (1981).

34. E. F. BERTAUT, *in* "Magnetism III" (G. T. Rado and H. Suhl, Eds.), Academic Press, New York (1963).

35. J. PEBLER, K. SCHMIDT, D. BABEL, AND W. VERSCHAREN, *Z. Naturforsch. B* **32**, 369 (1977).

36. P. IMBERT, G. JEHANNO, Y. MACHETEAU, AND F. VARRET, *J. Phys.* **37**, 969 (1976).

37. Y. LALIGANT, Y. CALAGE, E. TORRES-TAPIA, J. M. GRENECHE, F. VARRET, AND G. FEREY, *J. Magn. Magn. Mater.* **61**, 283 (1986).

38. G. HEGER, *Int. J. Magn.* **5**, 119 (1973).